

# **Generating negatively supercoiled DNA using dual-trap optical tweezers**

Graeme A. King,<sup>1#</sup> Dian Spakman,<sup>2</sup> Erwin. J.G. Peterman,<sup>2#</sup> and Gijs J.L. Wuite<sup>2#</sup>

<sup>1</sup> *Institute of Structural and Molecular Biology, University College London, Gower Street, London WC1E 6BT, UK*

<sup>2</sup> *Department of Physics and Astronomy, and LaserLaB Amsterdam, Vrije Universiteit Amsterdam, De Boelelaan 1081, 1081 HV, Amsterdam, The Netherlands*

# Correspondence should be addressed to: G.A. King (g.king@ucl.ac.uk), E.J.G. Peterman (e.j.g.peterman@vu.nl) or G.J.L. Wuite (g.j.l.wuite@vu.nl)

**Key words:** DNA supercoiling, Optical tweezers, DNA topology, DNA structure, Microfluidics

**Running head:** Supercoiling DNA using dual-trap optical tweezers

## **Abstract**

Many genomic processes lead to the formation of underwound (negatively supercoiled) or overwound (positively supercoiled) DNA. These DNA topological changes regulate the interactions of DNA-binding proteins, including transcription factors, architectural proteins and topoisomerases. In order to advance our understanding of the structure and interactions of supercoiled DNA, we recently developed a single-molecule approach called Optical DNA Supercoiling (ODS). This method enables rapid generation of negatively supercoiled DNA (with between <5% and 70% lower helical twist than non-supercoiled DNA) using a standard dual-trap optical tweezers instrument. ODS is advantageous as it allows for combined force spectroscopy, fluorescence imaging and spatial control of the supercoiled substrate, which is difficult to achieve with most other approaches. Here, we describe how to generate negatively supercoiled DNA using dual-trap optical tweezers. To this end, we provide detailed instructions on the design and preparation of suitable DNA substrates, as well as a step-by-step guide for how to control and calibrate the supercoiling density produced.

# 1 Introduction

The topological state of DNA *in vivo* is frequently altered by enzymes, such as polymerases, that lead to DNA overwinding (positive supercoiling) and underwinding (negative supercoiling) (1,2). The DNA linking number (the number of links between the two strands of a DNA molecule,  $Lk$ ) is decreased or increased, depending on whether negative or positive supercoiling is generated, respectively. Supercoiling plays a key regulatory role in many DNA-protein interactions (3,4). For example, negative supercoiling is sequestered through the formation of nucleosomes (in eukaryotes) and the binding of nucleoid associated proteins (in prokaryotes). Additionally, both positive and negative supercoiling can be relaxed by a range of topoisomerase enzymes (3,4). Together, these disparate processes contribute to supercoiling homeostasis in the cell and, on average, the genome of most organisms is slightly negatively supercoiled (5,6). Negative supercoiling has also been proposed to promote the binding of RNA guide sequences for CRISPR-Cas gene editing (7,8,9). Detailed mechanistic knowledge of the interplay between DNA supercoiling and DNA-binding proteins is therefore crucial for our understanding of genome biology.

Single-molecule methods, such as magnetic tweezers (7,9), micro-pipette tweezers (10) and angular optical trapping (11,12) have been used extensively to study the structure and biochemical interactions of supercoiled DNA (4,13). Although these assays allow both force and torsional stress to be applied to DNA, they can be difficult to combine with fluorescence imaging. Moreover, since the DNA molecule is tethered to a fixed surface, it cannot be physically moved within a flowcell. These features hinder the ability to visualize protein interactions on supercoiled DNA and perform rapid buffer exchanges. To address this, we recently developed an approach, called Optical DNA Supercoiling (ODS) (14), which enables rapid generation of negative supercoiling using dual-trap optical tweezers. Here, the supercoiled molecule is tethered between two optically-trapped beads, and by displacing one of the beads, a wide range of forces (typically 0.1-200 pN) can be applied to the DNA (15). Since the DNA molecule is oriented perpendicular to the microscope objective, the assay can be easily combined with fluorescence imaging (16,17). Additionally, both beads can be freely moved in solution, allowing the supercoiled molecule to be exchanged rapidly between different solutions within a multi-channel flowcell (18,19,20,21).

ODS exploits the intrinsic mechanical properties of DNA to generate a fixed reduction in  $Lk$  of between <5% and 70% relative to that of non-supercoiled (B-form) DNA. Although ODS is limited to the formation of negative, rather than positive, supercoiling, it can be readily implemented within a standard dual-trap optical tweezers instrument and therefore benefits from the many advantages of this platform. For example, ODS has previously been used to visualize structural transitions in underwound DNA and to demonstrate that negative supercoiling can regulate the diffusion dynamics of the mitochondrial transcription factor TFAM (14). In this chapter, we summarize the basic principle of ODS and the key

experimental considerations, and provide a step-by-step guide for how to generate underwound DNA using ODS.

### ***1.1 Principle of Optical DNA Supercoiling***

An end-closed DNA molecule is first tethered between two streptavidin-coated optically-trapped beads via at least two biotin moieties on each end of the DNA (see **Note 1** and Fig. 1A) (22). When more than one biotin-streptavidin linkage is formed between each end of the DNA molecule and a bead, the DNA is torsionally constrained, and thus  $Lk$  is fixed. Torsionally constrained DNA undergoes an overstretching transition at forces of  $\sim 115$  pN, during which the end-to-end length can increase by up to  $\sim 170\%$  of the contour length ( $Lc$ ) (Fig. 1B,C) (22,23). Although this transition results in local changes to the helical twist, the overall value of  $Lk$  remains unchanged (see **Note 2** and Fig. 1C). In contrast, when end-closed DNA is tethered to the beads via only one biotin-streptavidin bond on either end of the molecule, there is no torsional constraint. In this case, overstretching occurs at  $\sim 65$  pN and corresponds to a reduction in the overall  $Lk$  by up to  $\sim 70\%$  (see **Note 3** and Fig. 1B,D) (21,23). This change in  $Lk$  arises from swivelling of the DNA molecule around the single tether and is reversed upon reduction of the tension. From these observations, it can be appreciated that overstretching induces a torsional stress in DNA.

In ODS, the torsional stress induced within end-closed torsionally constrained DNA during overstretching is released (either partially or fully) through transient disruption of the biotin-streptavidin interactions. This results in at least one end of the DNA molecule being tethered to the beads via only a single biotin-streptavidin linkage for a brief period of time. During this time,  $Lk$  is reduced via swivelling of the DNA molecule around the single tether. Importantly, once the torsional stress has been (partially) released, the broken biotin-streptavidin bond(s) re-form (while the molecule is still overstretching). The molecule thus becomes torsionally constrained again, but with a lower  $Lk$  than that of non-supercoiled (B-form) DNA. Upon reduction of the tension, the DNA molecule retains the reduced  $Lk$  and is therefore preserved in a negatively supercoiled (underwound) state (14). Fig. 2A presents a schematic overview of the principle of ODS.

In addition to the mechanical properties of DNA, ODS relies on two critical features (14). The first is that the average lifetime of a biotin-streptavidin bond decreases exponentially as a function of tension (see **Note 4**) (24,25). As a result, the tethers can be transiently broken with high efficiency at high tensions (*e.g.*,  $>80$ - $100$  pN), but are stable at low tensions (*e.g.*,  $<40$  pN). The second feature is that, provided sufficiently large beads (*e.g.*,  $4.5$   $\mu\text{m}$  diameter) are employed, bead rotation in the optical traps is negligible (14,22). These features (see also **Note 5**) ensure that the negatively supercoiled state can be maintained at low forces over experimental timescales. For example, it has been demonstrated experimentally that for  $\lambda$ -DNA tethered between  $4.5$   $\mu\text{m}$  diameter beads, the fixed change in  $Lk$

generated using ODS is stable (*i.e.*, no detectable change in  $Lk$ ) over timescales more than 30 minutes at forces  $<40$  pN.

Since ODS is based on a stochastic process, the fixed change in  $Lk$  cannot be determined *a priori*. Nonetheless, the probability of a change in  $Lk$  can be tuned either by adjusting the applied force, the time held at high force or the relative change in DNA extension (as explained in detail in **Subheading 3.6**). In this way, it has been demonstrated that ODS can generate supercoiling densities ( $\sigma$ ) over a wide range (with  $\sigma$  between 0 and  $\sim -0.7$ ), as illustrated in Fig. 2B (**14**).  $\sigma$  represents the fractional change in  $Lk$ , relative to that of the non-supercoiled DNA molecule (*i.e.*,  $Lk-Lk_0/Lk_0$ , where  $Lk_0$  is the linking number of non-supercoiled DNA). The maximum value of  $\sigma$  generated with ODS reflects the maximum reduction in  $Lk$  attainable by overstressing torsionally unconstrained DNA (see **Note 6**). The magnitude of  $\sigma$  can be determined (with a maximum error of between 0.03 and 0.045) by comparison with published force-distance (FD-)curves of negatively supercoiled DNA (as detailed in **Subheading 3.8**) (**14**).

## ***1.2 Experimental considerations***

The diameter of the beads and the length of DNA used for ODS experiments should be considered carefully. The following considerations are most relevant.

1. Smaller beads have a lower drag coefficient, and thus increase the achievable force resolution due to lower Brownian noise on the measurement bandwidth (**16,26,27**).
2. Due to their lower drag coefficient, smaller beads have a higher rotational velocity under applied torque than larger beads (**14**), which could potentially result in (partial) loss of supercoiling through bead rotations.
3. The maximum force that can be applied without losing the bead from each trap decreases as a function of decreasing bead diameter (**28**). This is particularly relevant for ODS because forces greater than 115 pN are often required to generate a fixed change in  $Lk$ . The maximum force that can be applied to the beads can be increased by increasing the optical trapping laser power (**28**).
4. Higher laser powers can induce local heating (**14,29**), which can potentially disrupt the stability of the biotin-streptavidin interactions (**30**). Increased laser powers can also induce DNA damage (*e.g.*, nicks in the backbone). These latter two features can reduce the efficacy of ODS.
5. Larger beads (*e.g.*, 4.5  $\mu\text{m}$  diameter) ensure that the ends of the DNA molecule are far from the centre of the optical traps. This enhances the stability of the biotin-streptavidin interactions and minimizes photobleaching of proteins/ligands bound near the ends of the DNA molecule.

6. Although rotation of large diameter beads is negligible on experimental timescales (**14**), a small number of bead rotations would nonetheless have a much larger relative impact on the supercoiling density of a short DNA molecule compared with a long molecule.
7. Long DNA molecules are well-suited for fluorescence imaging of supercoiled DNA for three reasons. First, long DNA molecules allow the visualization of sequence-dependent binding of proteins/ligands (see **Note 7**). Second, photobleaching near the ends of the DNA (due to the trapping lasers) has a lower relative impact on the overall fluorescence intensity for a long DNA molecule compared with a shorter molecule. Third, the use of long DNA molecules minimizes the influence of background fluorescence from the beads (which can sometimes dominate the signal when using short DNA molecules).

For all of these reasons, we typically use 4.5  $\mu\text{m}$  diameter beads and  $\lambda$ -phage DNA (48.5 kb). However, it is likely that ODS can still be achieved using smaller beads (*e.g.*, 1-2  $\mu\text{m}$  diameter) by optimizing the laser power (for sufficient trapping force, but minimal photobleaching/local heating).

## 2. Materials

### 2.1 DNA construct preparation (see also Fig. 1A)

- 1  $\lambda$ -DNA (250 ng/ $\mu$ L, Roche).
- 2 End-cap 1 (100  $\mu$ M, Biolegio), with the following sequence:

5' *AGG TCG CCG CCC* **GGA GTT GAA CGT TTTT** ACG TTC AAC TCC 3'

This forms a hairpin structure consisting of a 5T-loop, a 12-bp double-stranded stem (bold), and a 12-nucleotide single-stranded (ss-)DNA overhang (italicized) (22). The latter is complementary to the left *cos* site of  $\lambda$ -DNA (31). Underlined bases are covalently linked to a biotin moiety.

- 3 End-cap 2 (100  $\mu$ M, Biolegio), with the following sequence:

5' *GGG CGG CGA CCT CAA GTT GGA CAA* TTTTT TTG TCC AAC TTG 3'

This forms a hairpin structure consisting of a 5T-loop, a 12-bp double-stranded stem (bold), and a 12-nucleotide ssDNA overhang (italicized) (22). The latter is complementary to the right *cos* site of  $\lambda$ -DNA (31). Underlined bases are covalently linked to a biotin moiety.

- 4 10x T4 DNA ligase buffer (ThermoFisher Scientific).
- 5 Polynucleotide kinase (10 units/ $\mu$ L, New England Biolabs).
- 6 T4 DNA ligase enzyme (5 units/ $\mu$ L, ThermoFisher Scientific).
- 7 MilliQ water.
- 8 Ice.
- 9 Temperature-controlled system for 0.5 mL and 1.5 mL tubes (16 - 80°C).

### 2.2 DNA purification

- 1 3 M Sodium Acetate.
- 2 Cold (-20°C) 96% (v/v) Ethanol.
- 3 Cold (-20°C) 70% (v/v) Ethanol.
- 4 Temperature-controlled (4°C) centrifuge for 1.5 mL tubes.
- 5 TE buffer (10 mM Tris-HCl, 1 mM EDTA, pH 8.5).

### 2.3 Core components for dual-trap optical tweezers set-up (Fig. 3)

1. Inverted microscope.
2. Automated microscope stage (MS-2000, Automated Scientific Instrumentation).
3. 60x water-immersion objective (Plan Apo, numerical aperture 1.2, Nikon).
4. Condenser top lens (P 1.40 OIL S1 11551004, Leica).

5. 1064 nm trapping laser, 10 W (YLR-10-LP, IPG Photonics).
6. Closed loop piezo mirror (NanoMTA2X, Mad City Labs).
7. Position sensitive detector (DL100-7PCBA3, Pacific Silicon Sensor).
8. LED (460 nm, Roithner Lasertechnik GmbH).
9. CMOS camera (DCC1545M, Thorlabs).

#### ***2.4 Microfluidic flow system (Fig. 4)***

1. Custom 5-channel glass flowcell (LUMICKS B.V.). See **Note 8**.
2. Tubing for entrance channels (1/16", Upchurch Scientific).
3. Exit tubing (1/32", Upchurch Scientific).
4. 5 syringes without needle (3 mL, Terumo).
5. Home-built syringe holder and pressure system that can apply up to 3 atm. to the solutions contained within each syringe in **step 4**.
6. Shut-off valves (Upchurch Scientific).
7. Waste vial (*e.g.*, 50 mL tube).

#### ***2.5 Cleaning of microfluidic flow system***

1. MilliQ water.
2. Household bleach (containing ~5% Sodium hypochlorite). See **Note 9**.
3. 0.5 M Sodium thiosulfate.
4. Single-edge razor blades.
5. Needle (size 26G).

#### ***2.6 Passivation of flowcell and tubing***

1. Phosphate Buffer Solution (PBS). This solution includes 5 mM  $\text{NaN}_3$  and 1 mM EDTA and is filter sterilized using a 0.2  $\mu\text{m}$  filter pore size.
2. Passivation buffer (PBS, 0.2% casein, 5 mM  $\text{NaN}_3$ , and 1 mM EDTA), filter sterilized using a 0.2  $\mu\text{m}$  filter pore size. See **Note 10**.
3. ODS buffer (20 mM Tris-HCl pH 7.5, 50 mM NaCl, 0.05% tween-20), filter sterilized using a 0.2  $\mu\text{m}$  filter pore size. See **Note 11**.

#### ***2.7 Reagents for single-molecule experiments***

1. Streptavidin-coated polystyrene beads solution (4.5  $\mu\text{m}$  diameter, 0.5% w/v, Spherotech). Referred to here as the 'Stock' beads solution.



2. Biotin-labelled end-capped  $\lambda$ -DNA solution (prepared using the reagents in **Subheading 2.1**).

### ***2.8 General materials***

- 1 Gloves (nitrile or similar).
- 2 Microcentrifuge tubes (0.5 mL and 1.5 mL).
- 3 Pipettes (P2, P20, P200, P1000).
- 4 Syringe filters with 0.2  $\mu\text{m}$  pore size (Whatman).
- 5 Syringes without needle (Terumo).
- 6 Sodium Azide.
- 7 EDTA.

### ***2.9 Data acquisition***

1. Custom (LabVIEW) software for control of optical tweezers instrumentation, power spectrum analysis, force detection and DNA end-to-end length determination.

### 3. Methods

#### 3.1 Generation of biotin-labelled end-capped DNA

The following steps describe how to generate end-closed  $\lambda$ -DNA substrates for ODS. Here, two end-caps (End-cap 1 and End-cap 2) are ligated to the two terminal cos sites of  $\lambda$ -DNA, respectively (14,22,32). Both of the end-caps, as well as the  $\lambda$ -DNA, are phosphorylated prior to ligation, and the ligated sample is purified using ethanol precipitation. The end-cap design and ligation strategy are illustrated schematically in Fig. 1A.

##### 3.1.1 Phosphorylation of DNA

1. Add 5.5  $\mu$ L of 10x T4 DNA ligase buffer to 50  $\mu$ L of  $\lambda$ -DNA (250 ng/ $\mu$ L) in a 1.5 mL microcentrifuge tube and mix gently (see **Note 12**). To this, add 0.5  $\mu$ L of polynucleotide kinase (10 units/ $\mu$ L) and incubate at 37°C for one hour.
2. Add 2  $\mu$ L of 10x T4 DNA ligase buffer to 15.5  $\mu$ L of MilliQ water in a 0.5 mL microcentrifuge tube, followed by 2  $\mu$ L of End-cap 1 (100  $\mu$ M) and mix gently. To this, add 0.5  $\mu$ L of polynucleotide kinase (10 units/ $\mu$ L) and incubate at 37°C for one hour.
3. Add 2  $\mu$ L of 10x T4 DNA ligase buffer to 15.5  $\mu$ L of MilliQ water in a 0.5 mL microcentrifuge tube, followed by 2  $\mu$ L of End-cap 2 (100  $\mu$ M) and mix gently. To this, add 0.5  $\mu$ L of polynucleotide kinase (10 units/ $\mu$ L) and incubate at 37°C for one hour.

##### 3.1.2 Ligation of phosphorylated DNA segments

1. Add 51  $\mu$ L of 10x T4 DNA ligase buffer to 400  $\mu$ L of MilliQ water in a 1.5 mL microcentrifuge tube and mix gently. To this, add 56  $\mu$ L of phosphorylated  $\lambda$ -DNA (14 nM, prepared in **Subheading 3.1.1**) and 1  $\mu$ L of phosphorylated End-cap 1 (10  $\mu$ M, prepared in **Subheading 3.1.1**). See **Notes 12** and **13**.
2. Incubate the solution at 80°C for five minutes and then place on ice (see **Note 14**).
3. Add 2  $\mu$ L of T4 DNA ligase enzyme (5 units/ $\mu$ L) to the above solution and incubate at 16°C for 8-12 hours.
4. Add 10  $\mu$ L of phosphorylated End-cap 2 (10  $\mu$ M, prepared in **Subheading 3.1.1**) to the above solution.
5. Incubate the solution at 80°C for five minutes and then place on ice.
6. Add 2  $\mu$ L of T4 DNA ligase enzyme (5 units/ $\mu$ L) to the above solution and incubate at 16°C for 8-12 hours.

##### 3.1.3 DNA purification

1. Split the 522  $\mu\text{L}$  solution prepared in **steps 1-6** in **Subheading 3.1.2** into two, by slowly pipetting 261  $\mu\text{L}$  of this solution into a new 1.5 mL microcentrifuge tube, leaving the remaining 261  $\mu\text{L}$  in the original tube.
2. To each microcentrifuge tube above, add 26.1  $\mu\text{L}$  (0.1 reaction volume) of 3 M Sodium Acetate and 653  $\mu\text{L}$  (2.5 reaction volume) of cold ( $-20^{\circ}\text{C}$ ) 96% (v/v) ethanol. Mix by slowly inverting the tubes 3 times, taking care not to vortex.
3. Incubate the above solutions at  $-20^{\circ}\text{C}$  overnight (longer incubation periods are also fine).
4. Centrifuge for 30 min at 12,000 x  $g$  at  $4^{\circ}\text{C}$ .
5. Remove the ethanol from each tube by tipping it into empty microcentrifuge tubes. A small pellet of DNA is usually visible on the side of the reaction tubes after ethanol removal.
6. Add 0.7 mL of cold ( $-20^{\circ}\text{C}$ ) 70% (v/v) ethanol slowly to each of the tubes that contain a DNA pellet. Try to direct the ethanol onto the side of the tube that is opposite to where the pellet lies (in order to avoid disrupting the pellet). Do not mix after adding the ethanol.
7. Centrifuge the solutions for 10 min at 12,000 x  $g$  at  $4^{\circ}\text{C}$ .
8. Remove the ethanol from each tube by tipping it into empty microcentrifuge tubes. Again, a small pellet of DNA is typically visible on the side of the tube after ethanol removal. Leave the tubes containing the DNA pellets open on the bench for 10 minutes or until most of the residual ethanol has evaporated. However, do not dry completely as this could damage the DNA.
9. Resuspend the pellet of DNA in 200  $\mu\text{L}$  TE buffer (or until the pellet is fully submerged).
10. The resuspended DNA solution, referred to henceforth as the 'Purified end-capped DNA solution' can be stored at  $4^{\circ}\text{C}$  for many months (see **Notes 15** and **16**).

### ***3.2 Optical trapping instrumentation***

ODS experiments are performed using a dual-trap optical tweezers instrument based on an inverted microscope design that has been described in detail previously (Fig. 3) (**18**). The core elements of this design are as follows.

1. Two orthogonally polarized optical traps (termed here Trap 1 and Trap 2) are generated by splitting a 1064 nm laser beam into two independently steerable laser paths. The two optical traps can be selectively blocked using computer-controlled laser beam blockers.
2. Trap 1 and Trap 2 are each used to catch a single streptavidin-coated polystyrene bead (termed here Bead 1 and Bead 2, respectively) within the multi-channel flowcell mounted on an automated  $xy$ -stage. A single DNA molecule is then tethered between these two beads.

3. The position of Trap 2 / Bead 2 in the focal plane is controlled with absolute positioning (over a range of  $\sim 20 \mu\text{m}$  in the  $x$ -direction and  $\sim 10 \mu\text{m}$  in the  $y$ -direction) using a mirror mounted on a piezo stage. The position of Trap 1 can be controlled using a mirror mounted on a stepper-motor stage. For ODS experiments, the position of Trap 2 / Bead 2 is displaced, while the position of Trap 1 / Bead 1 is held stationary.
4. The force on Bead 1 is measured using back-focal plane interferometry based on the light from Trap 1. Here, the back-focal plane of the condenser top lens is imaged onto a position-sensitive detector (PSD) and the force applied to Bead 1 is determined using the output voltage of the PSD (33). The output voltage depends directly on the intensity distribution, which in turn depends on the force applied to the bead and the trap stiffness.
5. The force is calibrated by recording a power spectrum of the thermal fluctuations of Bead 1 (in Trap 1) obtained from the PSD signal. The pN/V and trap stiffness values are obtained by fitting a Lorentzian function to the power spectrum (34).
6. The trapped beads are imaged using brightfield microscopy, by illuminating with a 460 nm LED and collecting the transmitted light on a CMOS camera. The end-to-end length of the DNA molecule is determined by measuring the distance between the two trapped beads based on their brightfield images.
7. The optical trapping hardware (including steerable mirrors, laser beam blockers and microscope stage) is controlled using a custom-written LabVIEW program. This program is additionally used to calibrate the force and track the bead positions.

### ***3.3 Microfluidic flow system***

ODS experiments are conducted within a multi-channel flowcell, which is connected to a pressure system, as illustrated schematically in Fig. 4. In our configuration, the flowcell has a custom-made glass design with 5 inlet channels (labelled Channels 1-5), which are each connected to inlet tubing via holes in the upper glass surface. Channels 1-3 physically merge near the upstream end of the flowcell to create a central chamber. Channels 4 and 5 are connected to the central chamber further downstream (as outlined in Fig. 4, inset). Exit tubing (connected to the downstream end of the central chamber via a hole in the upper glass surface) allows fluids to be flowed through the flowcell towards a waste vial. The contents of Channels 1-3 are separated in the central chamber through laminar flow. Solutions to be added to Channels 1-5 are stored in syringes (labelled Syringes 1-5) which are connected, respectively, to the inlet tubing via valves (labelled Valves 1-5). The syringes are held within a home-made pressure box that allows application of up to 3 atm. For ODS experiments, it is vital that there are no blockages in the system (these can sometimes form at the ends of the tubing and within the valves due to salt deposits or other microscopic residues). Blockages can potentially generate shear forces on the DNA that can induce backbone

damage (*i.e.*, nicks). The presence of a single nick in the tethered DNA molecule results in a loss of torsional constraint and therefore prevents ODS from being performed. It is also important that the flowcell system is thoroughly cleaned before starting experiments, to prevent contamination from either inert microscopic particles or bacteria. These contaminants can often become caught in the optical traps, and thus perturb the force calibration. Additionally, bacteria can produce biochemicals that nick the DNA. Finally, in the event that proteins will be added to the flowcell, the surface of the channels and tubing should be passivated with a blocking agent to prevent the proteins from binding to the surfaces (see **Note 17**). Below we describe protocols for (i) removing blockages, (ii) cleaning the flow system, (iii) passivating the flow system and (iv) preparing samples for ODS experiments.

### ***3.3.1 Checking for blockages in the flow system***

1. Add ~1 mL of MilliQ water to each inlet syringe and apply a high pressure.
2. Check that the rate of fluid flow through all channels is similar. If this is not the case, there is most likely a blockage in either the tubing or one of the valves. Blockages in the tubing can usually be removed by cutting ~2 mm off the end using a clean razor blade. Blockages in the valves can be removed by disconnecting the tubing and either (a) flowing water at maximum pressure through the valve or (b) dislodging any blockages with a needle.

### ***3.3.2 Cleaning the flow system***

1. Add ~1 mL of common bleach (containing ~5% sodium hypochlorite solution) to each inlet syringe and flush through the flowcell over a period of 15-20 minutes.
2. Add ~1 mL of MilliQ water to each inlet syringe and flush through the flowcell rapidly.
3. Add ~1 mL of MilliQ water once more to each inlet syringe. To this, add 3-4 drops of 0.5 M sodium thiosulfate (see **Note 18**). Flush this solution through the flowcell over a period of ~10 minutes.
4. Add ~1 mL of MilliQ water to each inlet syringe and flush through the flowcell rapidly. Repeat this step 2-3 times to ensure all residual bleach and/or sodium thiosulfate has been removed.

### ***3.3.3 Passivation***

1. Add ~1 mL of filtered PBS to each inlet syringe and flow rapidly through the flowcell.
2. Add ~1 mL of filtered Passivation buffer to each inlet syringe. Flow these solutions simultaneously through the flowcell slowly over a period of at least 20-30 minutes. Ensure there are no air bubbles in the flowcell during and after passivation (see **Note 19**).

3. Add ~1 mL of filtered ODS buffer to each inlet syringe and flow through the flowcell. Repeat 1-2 times to ensure there are no casein aggregates remaining in solution in the flowcell.

#### ***3.3.4 ODS Sample preparation***

1. Prepare a 'Working Beads' solution by adding 10  $\mu$ L of the 'Stock' Beads solution (see **step 1, Subheading 2.7**) to a microcentrifuge tube containing 1 mL of filtered ODS buffer.
2. Prepare a 'Working DNA' solution by adding between 1  $\mu$ L and 5  $\mu$ L of the Purified end-capped DNA solution (prepared in **Subheading 3.1.3**) to a microcentrifuge tube containing 1 mL of filtered ODS buffer (See **Note 20**). Pipetting should be performed slowly and gently.

#### ***3.4 Tethering DNA between optically-trapped beads***

The first stage of an ODS experiment is to tether a single DNA molecule between two optically-trapped beads, using the following protocol.

1. Mount the cleaned and passivated flowcell on the microscope stage.
2. Place water on the objective, and immersion oil on the upper surface of the flowcell.
3. Adjust the objective height such that it is focussed on the middle of the flowcell.
4. Insert (i) 0.5-1 mL of the 'Working Beads' solution (prepared in **step 1 in Subheading 3.3.4**) into Syringe 1, (ii) 0.5-1 mL of the 'Working DNA' solution (prepared in **step 2 in Subheading 3.3.4**) into Syringe 2 and (iii) 0.5-1 mL of filtered ODS buffer into Syringe 3. Note that ODS experiments can be performed efficiently in this buffer (see **Note 21**). To the remaining syringes, add 0.5-1 mL of either ODS buffer or an alternative buffer. Proteins and/or DNA-binding ligands (such as intercalator dye) can be added to the solutions in Syringes 4 and 5, if desired.
5. Open all inlet syringe valves and apply pressure to generate fluid flow through the flowcell.
6. Flush ~0.2 mL of fluid from the syringes through the flowcell. Then reduce the flow speed to a minimum.
7. Open the optical trapping laser beam shutters.
8. Position the optical traps within Channel 1, and catch a single bead in each trap (see **Note 22**). Adjust the fluid flow, if necessary, to maximize the probability of catching a bead in each optical trap.
9. Move the optically-trapped beads to Channel 3 and stop the fluid flow by closing all inlet syringe valves. Next, calibrate the force on Bead 1 (see **steps 4-5, Subheading 3.2**) (**34**).

10. Position the trapped beads such that the distance between the nearest edges of Bead 1 and Bead 2 (defined here as  $D_B$ ) is  $\sim 11 \mu\text{m}$  (See Fig. 2A and **Note 23**). This corresponds to  $\sim 67\%$  of  $L_c$  for  $\lambda$ -DNA). Open the inlet syringe valves and apply a gentle fluid flow such that the drag force on Bead 1 is between 40 pN and 100 pN. Then move the beads to Channel 2 in order to tether DNA between the two beads.
11. After 10-15 seconds in Channel 2 (see **Note 24**), move the beads to Channel 3 and minimize the fluid flow.
12. Check if DNA is tethered between the two beads by moving Bead 2 until  $D_B$  is  $\sim 16.3 \mu\text{m}$  (corresponding to  $L_c$  for  $\lambda$ -DNA). If no increase in force is detected, there is no DNA tethered between the beads. In this event, **steps 10-11** should be repeated until tethered DNA is detected.
13. Once DNA is successfully tethered between the two beads, close all inlet syringe valves.

### ***3.5 Testing the DNA integrity***

The next stage is to check that the tethered DNA is torsionally constrained, which can be achieved as follows.

1. Position the trapped beads such that  $D_B$  is  $\sim 11 \mu\text{m}$  and set the force on Bead 1 to 0 pN.
2. Stretch the DNA molecule by increasing  $D_B$  (via displacing Bead 2), until the force measured on Bead 1 reaches  $\sim 65$  pN.
3. If the recorded FD-curve exhibits an ‘overstretching’ plateau at  $\sim 65$  pN, the molecule is not torsionally constrained. If this is the case, continue overstretching until the end-to-end length is at least  $\sim 18\text{-}20 \mu\text{m}$  ( $\sim 1.15 L_c$  for  $\lambda$ -DNA). Then reduce  $D_B$  to  $\sim 11 \mu\text{m}$ . If the extension FD-curve exhibits a non-smooth force plateau at  $\sim 65$  pN and/or there is significant hysteresis between the extension and retraction FD-curves, the DNA is nicked (Fig. 5A). Alternatively, if the extension FD-curve exhibits a smooth force plateau at  $\sim 65$  pN and there is negligible hysteresis between the extension and retraction FD-curves, the DNA is torsionally unconstrained, but not nicked (Figs. 1D and 5B).
4. If the DNA molecule is nicked, dispose of the beads (by transiently closing the optical trapping laser beam shutters), and repeat **steps 7-13** in **Subheading 3.4** until a non-nicked DNA molecule is tethered between the two beads. For efficient generation of underwound DNA using ODS, ensure that the fraction of nicked DNA molecules is no more than 30% (see **Note 25**). If  $>30\%$  of DNA molecules are nicked, check if there are air bubbles in the flowcell or blockages in the tubing (which can induce nicks). See **Note 26**.

5. If the force measured on Bead 1 reaches  $>75$  pN for DNA end-to-end lengths  $>1.1 L_c$ , the DNA molecule is torsionally constrained (See **Note 27**). ODS can be performed on these molecules.

### ***3.6 Performing an ODS experiment***

The manner in which a fixed reduction in  $Lk$  is generated in end-closed torsionally constrained DNA via ODS can be divided into three general categories, referred to here as Type 1, Type 2 and Type 3, respectively. The difference between these categories lies in the ease with which the biotin-streptavidin bonds can be transiently disrupted under applied tension, with the following characteristics (see also Fig. 6).

Type 1 molecules display a smooth plateau in the FD-curve centred at  $\sim 115$  pN between  $\sim 1.15 L_c$  and  $1.7 L_c$ , similar to that reported previously for non-supercoiled torsionally constrained DNA (22,23). In most cases, a fixed reduction in  $Lk$  usually occurs only at end-to-end lengths  $>1.75 L_c$  (*i.e.*, beyond the end of the overstretching transition). This is highlighted in Fig. 6A,B. The magnitude of the reduced  $Lk$  generated by ODS in Type 1 molecules is proportional to both the force applied and the duration at high force (14).

Type 2 molecules give rise to an FD-curve that exhibits large, and sudden, force ruptures between  $\sim 1.1 L_c$  and  $1.75 L_c$ . The maximum force of these ruptures is  $\sim 115$  pN, corresponding to the force plateau expected for non-supercoiled torsionally constrained DNA. The sudden decrease in force during each rupture arises from transient loss of a biotin-streptavidin linkage, resulting in a fixed reduction in  $Lk$ . The force then rises again as the end-to-end length is increased further. The fixed reduction in  $Lk$  generated in these molecules is directly proportional to the distance at which the force rupture occurs (see Fig. 6C,D) (14).

Type 3 molecules exhibit a rough (*i.e.*, non-smooth) force plateau in the FD-curve between  $\sim 80$  pN and  $100$  pN as the end-to-end length is increased from  $\sim 1.1 L_c$  to  $1.75 L_c$ . This distinctive behaviour arises from frequent transient loss of a biotin-streptavidin linkage upon progressively increasing the end-to-end length. The fixed reduction in  $Lk$  generated in these molecules is directly proportional to the extent to which the DNA molecule is extended (over the range of  $\sim 1.1 L_c$  to  $1.75 L_c$ ), and in most cases, the maximum possible supercoiling density ( $\sigma \sim -0.7$ ) is formed at  $\sim 1.75 L_c$  (14). See Fig. 6E,F.

By exploiting the specific characteristics of these three behaviours (see **Note 28**), ODS can be used to generate, and select for, supercoiling densities across a wide range (with  $\sigma$  between 0 and  $-0.7$ ) using the following protocols.

#### ***3.6.1 Generating underwound DNA using Type 1 end-closed torsionally constrained DNA substrates***



1. Set  $D_B$  to  $\sim 11 \mu\text{m}$ .
2. Calibrate the force on Bead 1, as described in **steps 4-5** in **Subheading 3.2**.
3. Set the force on Bead 1 to 0 pN.
4. Extend the DNA molecule by increasing  $D_B$ , via displacement of Bead 2, until the force measured on Bead 1 reaches  $\sim 150$  pN. Wait for 10 seconds at this force before decreasing  $D_B$  by moving Bead 2 back to its initial position.
5. Compare the extension and retraction FD-curves. If a fixed reduction in  $Lk$  occurred prior to retraction, the retraction curve will display features consistent with the FD-curve of underwound DNA (*e.g.*, with a force plateau at  $\sim 55$  pN, see Fig. 2B). On average, a single stretch-retract cycle as described in **step 4** leads to a small change in  $Lk$  (corresponding to a value of  $\sigma$  between 0 and  $-0.05$ ) (**14**).
6. Repeat **step 4** until the desired change in  $Lk$  is obtained. On average,  $\sim 10$ - $12$  repeats will yield the maximum possible change in  $Lk$  (*i.e.*,  $\sigma \sim -0.7$ ).
7. In a subset of molecules, repeated cycles of **step 4** will only lead to small changes in  $Lk$ . In these cases, larger changes in  $Lk$  can often be induced by either increasing the force further (*e.g.*, to  $>180$  pN) or increasing the time that the molecule is held at 150 pN for. Note that, if required, temporarily increasing the optical trapping laser power can also promote a change in  $Lk$  (by de-stabilizing the biotin-streptavidin interactions, see **Subheading 1.2**).
8. In a small fraction of cases (usually no more than 20%), no change in  $Lk$  can be achieved within 1 minute at tensions  $>180$  pN. In such cases, it is highly likely that the tethering of the DNA molecule to the beads will break completely before a change in  $Lk$  can be achieved. If no change in  $Lk$  can be generated, dispose of the beads, trap two new beads and tether a fresh DNA molecule between them, as described in **steps 7-13** in **Subheading 3.4**.

### **3.6.2 Generating underwound DNA using Type 2 end-closed torsionally constrained DNA substrates**

1. Set  $D_B$  to  $\sim 11 \mu\text{m}$ .
2. Calibrate the force on Bead 1, as described in **steps 4-5** in **Subheading 3.2**.
3. Set the force on Bead 1 to 0 pN.
4. Extend the DNA molecule by increasing  $D_B$ , via displacement of Bead 2, until the first force rupture is observed. The end-to-end length at which this occurs is referred to here as  $D_{\text{rupture}}$ . Immediately decrease  $D_B$  by moving Bead 2 back to its initial position.
5. The fixed reduction in  $Lk$  achieved in **step 4** is directly proportional to  $D_{\text{rupture}}$ .

6. If **step 4** yields the desired reduction in  $Lk$ , the DNA molecule can be directly used for further single-molecule experiments. If, however, a greater reduction in  $Lk$  is required, repeat **step 4**. Upon each repeat of **step 4**, the first force rupture will occur at progressively larger values of  $D_B$  until the maximum reduction in  $Lk$  (i.e.,  $\sigma \sim -0.7$ ) is achieved.

### **3.6.3 Generating underwound DNA using Type 3 end-closed torsionally constrained DNA substrates**

1. Set  $D_B$  to 11  $\mu\text{m}$ .
2. Calibrate the force on Bead 1, as described in **steps 4-5** in **Subheading 3.2**.
3. Set the force on Bead 1 to 0 pN.
4. Extend the DNA molecule by increasing  $D_B$ , via displacement of Bead 2, until the end-to-end length is  $\sim 1.1 Lc$ . Immediately decrease  $D_B$  by moving Bead 2 back to its initial position. This will result in a small fixed reduction in  $Lk$  ( $\sigma \sim -0.05$ ).
5. Repeat **step 4**, each time extending the molecule to increasing end-to-end lengths until the desired fixed change in  $Lk$  is achieved. When using Type 3 molecules, if a high supercoiling density is required, it is recommended to perform many stretch-retract cycles, with each cycle extending progressively further from  $\sim 1.1 Lc$  to  $1.75 Lc$ . This is because extending Type 3 molecules immediately to  $\sim 1.75 Lc$  can often lead to complete rupture of the biotin-streptavidin linkages, and thus loss of the DNA molecule.

### **3.6.4 Generating a fixed reduction in $Lk$ when starting with torsionally unconstrained end-closed DNA**

In  $\sim 10$ - $15\%$  of cases, the DNA molecule contains no nicks, but is torsionally unconstrained, owing to the presence of a single biotin-streptavidin bond on at least one end of the DNA molecule, even at low forces (see **step 3** in **Subheading 3.5**). Approximately  $50\%$  of these molecules can be converted to a torsionally constrained state using the following approach (see **Note 29** and Fig. 7).

1. Set  $D_B$  to  $\sim 11 \mu\text{m}$ .
2. Calibrate the force on Bead 1, as described in **steps 4-5** in **Subheading 3.2**.
3. Set the force on Bead 1 to 0 pN.
4. Extend the DNA molecule by increasing  $D_B$ , via displacement of Bead 2, until the end-to-end length is  $\gg 1.75 Lc$ . Deliberately break the tethering between the DNA molecule and one of the beads.

5. With  $D_B$  still greater than  $1.75 Lc$ , open the valve connecting Syringe 3 to Channel 3 and apply sufficient buffer flow within Channel 3 such that the drag force on Bead 1 is around 80-100 pN.
6. Bring Bead 2 progressively closer to Bead 1 until  $D_B$  is  $\sim 11 \mu\text{m}$ .
7. Close the valve.
8. Set the force on Bead 1 to 0 pN.
9. Extend the DNA molecule by increasing  $D_B$ , via displacement of Bead 2, until  $D_B$  is equivalent to  $\sim 1.1 Lc$ . If either no DNA is present, or the DNA is still torsionally unconstrained, dispose of the beads. Often, however, the same DNA molecule probed in **step 4** can be re-tethered but will now be torsionally constrained (due to the binding of two or more biotin moieties to both beads). If this occurs, a fixed reduction in  $Lk$  can be generated as described in **Subheadings 3.6.1 – 3.6.3**, depending on whether the molecule is characterized as Type 1, 2 or 3, respectively.

### ***3.7 Testing the temporal stability of the reduced $Lk$***

The vast majority (at least 90%) of negatively supercoiled molecules generated with ODS display no significant change in  $Lk$  at forces  $< 40$  pN over timescales  $> 30$  minutes (**14**). However, a small subset can sometimes lose their supercoiling density due to spontaneous disruption of the biotin-streptavidin interactions, even at low forces. These ‘unstable’ molecules should be identified (using the following protocol) and discarded. If the fixed reduction in  $Lk$  is stable over a period of  $\sim 2$  minutes at low force, it is usually also stable over much longer time frames (hours).

1. After confirming the formation of negatively supercoiled DNA based on the retraction FD-curve (see **Subheadings 3.6.1 – 3.6.3**), immediately record a subsequent extension FD-curve, by moving Bead 2 until the force measured on Bead 1 reaches  $\sim 70$  pN.
2. Decrease  $D_B$  to  $\sim 11 \mu\text{m}$  by moving Bead 2 and wait for at least two minutes.
3. Re-extend the DNA molecule by displacement of Bead 2 until the force measured on Bead 1 reaches  $\sim 70$  pN.
4. If there is any significant change in  $Lk$  as determined by comparing the two FD-curves in **steps 1 and 3**, dispose of the beads, trap two new beads and perform ODS on a new DNA molecule, as outlined in **Subheadings 3.4 – 3.6**. If there is no difference in the extension FD-curve recorded in **step 3** compared with that obtained in **step 1**, the supercoiling density is stable and the molecule can be used reliably for further study. For example, it can be safely transferred to other channels in the flowcell, where it can be incubated in a wide range of salt and/or protein solutions (see **Note 30**).

### 3.8 Calibrating the fixed change in $Lk$

The magnitude of  $Lk$  generated using ODS cannot be measured directly. However, it can be determined indirectly by comparing the recorded FD-curve of the supercoiled molecule with FD-curves of known supercoiling densities (the latter measured independently) using the following protocol (**14**).

1. Reference FD-curves for a series of known supercoiling densities are obtained. These can either be recorded in-house (using magnetic tweezers or another force-spectroscopy method with direct twist control) or derived from literature. In our case, we use FD-curves for supercoiled DNA reported previously by Léger *et al* (**23**).
2. For each supercoiling density associated with the reference FD-curves (*e.g.*, from literature), determine the DNA end-to-end length at 70 pN. Then calculate the difference between this value and the end-to-end length of non-supercoiled torsionally constrained DNA at 70 pN. This difference is referred to here as  $\Delta L_{70\text{pN}}$  ( $\Delta L_{70\text{pN}}$  is shown schematically in Fig. 8A).
3. Plot  $\Delta L_{70\text{pN}}$  against the supercoiling density and fit the data points with a linear function. The linear function serves as a calibration tool for ODS-derived FD-curves (Fig. 8B).
4. For each supercoiled molecule generated using ODS, record an FD-curve up to 70 pN. From this curve, determine  $\Delta L_{70\text{pN}}$  (as shown in Fig. 8A). Identify the supercoiling density associated with this value of  $\Delta L_{70\text{pN}}$  in the calibration plot (constructed in **step 3**). In this way, the magnitude of  $\sigma$  for any supercoiled molecule generated via ODS can be estimated. To minimize errors, ensure that the ODS-derived FD-curve is recorded under similar buffer/salt conditions as those curves used to construct the calibration plot in **step 3**. See **Note 31**.

## Notes

1. In our design of end-closed DNA (Fig. 1A), each end is labelled with four biotin moieties. Due to steric constraint, it is unlikely that all four biotins bind to the streptavidin-coated beads at the same time. However, in the majority of cases (~85-90%), at least two biotin moieties are tethered to each bead at any one time at low forces.
2. When a torsionally constrained DNA molecule is overstretched, it adopts a heterogeneous extended structure, in which ~80% of the molecule is underwound and the remaining ~20% is overwound (Fig. 1C) (22,23). The underwound regions can be either basepair melted (bubbles) or basepaired (in the form of S-DNA), depending on the salt concentration and other environmental conditions (22). S-DNA has been predicted to exhibit a helicity of ~37.5 bp/turn (23). The overwound regions are thought to adopt a P-DNA conformation, which is ~60-70% longer than B-DNA and has a twist of ~2.5 bp/turn. In P-DNA, the two backbones are tightly entwined, with the bases flipped to the outside (23,35).
3. In the absence of torsional constraint, overstretching of end-closed DNA corresponds to a cooperative transition from B-DNA to an extended underwound form (Fig. 1D). The underwound structure can be either basepair melted (bubbles) or basepaired (in the form of S-DNA) (21). See **Note 2**.
4. Theoretical calculations, supported by experimental studies, predict that the average lifetime of a biotin-streptavidin bond is <10 seconds at forces >100 pN, and >10<sup>5</sup> seconds at forces <10 pN (24,25).
5. ODS could, in principle, also be implemented with other single-molecule manipulation techniques. The key requirements are that (a) sufficient tensions (at least 115 pN) can be applied to induce transient biotin-streptavidin disruption and (b) large beads (*e.g.*, 4.5 μm diameter) and long DNA molecules (*e.g.*, λ-DNA) are used to ensure no loss of supercoiling through bead rotations.
6. The maximum supercoiling density that can be generated using ODS is dictated by the extent to which torsionally unconstrained DNA can be underwound by applied tension. For end-closed unconstrained DNA that is fully overstretched (*i.e.*, with an end-to-end length of ~1.75  $L_c$ ), the twist throughout the molecule is ~37.5 bp/turn (see **Note 2**). Since the tension rises sharply when the end-to-end length of torsionally unconstrained DNA is increased beyond ~1.75  $L_c$ , it is difficult to induce further unwinding beyond ~37.5 bp/turn. Thus, if an end-closed torsionally constrained DNA molecule loses torsional constraint for sufficient time at ~1.75  $L_c$ , the DNA molecule will adopt a helicity of ~37.5 bp/turn throughout its length. If the disrupted biotin-streptavidin bonds subsequently re-form, and the tension is reduced, the DNA molecule will be negatively supercoiled, with  $Lk \sim \text{number of bp} / 37.5$ . Non-supercoiled B-

form DNA exhibits an  $Lk$  ( $Lk_0$ ) of  $\sim$  number of bp / 10.5 (since B-DNA has a helicity of  $\sim$ 10.5 bp/turn). Consequently, the maximum possible value of  $\sigma$  ( $=\Delta Lk/Lk_0$ ) =  $\sim$ -0.72 (**14**).

7. When probing the sequence binding preferences of proteins/ligands on negatively supercoiled DNA, it can be advantageous to know the orientation of the DNA molecule. This orientation cannot be determined directly using the substrate design shown in Fig. 1A. However, the orientation could be determined by covalently linking a fluorescent dye near one end of the DNA molecule, by analogy with that used in other single-molecule imaging experiments (**36**).
8. A minimum of three inlet channels are required in order to introduce beads, DNA and buffer separately into the flowcell, but having more than 3 channels allows the DNA molecule to be moved rapidly between different buffer/protein/ligand solutions. Flowcells can also be constructed manually using a glass slide and a coverslip separated by a layer of parafilm or adhesive tape containing pre-cut channels (**37**).
9. ‘Thin’ rather than ‘thick’ household bleach is used for flowcell cleaning as thick bleach can be too viscous and clog the tubing.
10. 0.2% casein is prepared by diluting a 1% w/v ‘stock’ casein solution in PBS. The stock casein solution is prepared by gently dissolving casein powder in PBS containing 5 mM  $\text{NaN}_3$  and 1 mM EDTA. If handled carefully (*e.g.*, using gloves and avoiding leaving the solution open to air for long periods of time), the stock casein solution can be stored at room temperature for several months without degrading.
11. ODS buffer solutions used for single-molecule experiments are prepared freshly on the day that experiments are to be conducted, by diluting a pre-prepared high concentration ‘stock’ buffer solution (*e.g.*, 500 mM Tris-HCl, pH 7.5). To prevent bacterial growth, all stock buffer solutions contain 1 mM EDTA and 5 mM  $\text{NaN}_3$  and are stored in a fridge.
12. It is important not to shake, vortex or abruptly mix solutions containing DNA, as these mechanical actions can induce DNA backbone damages. These nicks will prevent the tethered DNA from being torsionally constrained and thus ODS cannot be performed.
13. Whenever pipetting DNA (especially longer DNA molecules, such as  $\lambda$ -DNA), this should be performed slowly and gently to avoid applying shear forces that can induce DNA backbone damages (*i.e.*, nicks).
14. Heating the DNA solution to 80°C followed by rapid cooling on ice ensures that each end-cap anneals to the complementary overhang of  $\lambda$ -DNA in its minimum energy conformation. The duration at 80°C is limited to 5 minutes to minimize thermal-induced DNA backbone damage.
15. Purified end-capped DNA can be stored in a fridge for many months without degrading (*i.e.*, without developing backbone nicks) provided the following precautions are taken. (i) Gloves (nitrile or similar) should be worn whenever handling the sample to avoid contamination with

DNAases or bacteria that can degrade the DNA. (ii) For similar reasons, the microcentrifuge tube containing the sample should not be left with the lid open for long periods of time. (iii) Care should be taken not to mix or vortex the sample to prevent mechanical-induced damage to the DNA. (iv) To further minimize degradation of the DNA, it can be advantageous to aliquot the stock sample into smaller (*e.g.*, 50  $\mu\text{L}$ ) samples.

16. Ethanol precipitation usually has a yield of between 50% and 100%. Thus, for stock solutions that are prepared by resuspending the DNA in 200  $\mu\text{L}$  TE buffer (in **step 9, Subheading 3.1.3**), a DNA concentration of 15-30 ng/ $\mu\text{L}$  is normally obtained.
17. Proteins in solution readily bind non-specifically to the surfaces of the flowcell system, which can result in depletion of the local protein concentration. This can be minimized by passivating the surfaces with blocking agents such as casein, BSA (often in combination with Pluronics) or lipid bilayers. Casein and BSA-Pluronics are both well-suited for passivating glass and plastic surfaces (*e.g.*, tubing), while lipid bilayers should only be used for passivating glass surfaces (**38**).
18. Sodium thiosulfate degrades residual bleach in the flowcell (**38**).
19. Air bubbles in the flowcell can cause local fluid mixing that can result in shear forces on the DNA, leading to DNA backbone damage. Air bubbles can be removed using rapid fluid flow. This can be achieved by either (a) application of high pressure on the inlet syringe pumps or (b) suction using a syringe connected to the exit tubing of the flowcell (see Fig. 4).
20. The optimal DNA concentration for ODS experiments is one that allows a single DNA molecule to be tethered between the two beads after incubation in Channel 2 for 10-15 seconds under modest buffer flow. If the concentration is too high, more than one DNA molecule will be tethered between the two beads, which can restrict controlled generation of negative supercoiling. For Purified end-capped DNA solutions that are prepared by resuspending the DNA pellet in 200  $\mu\text{L}$  of TE buffer (in **step 9, Subheading 3.1.3**), a 1000-fold dilution is usually optimal for tethering the DNA between beads in the flowcell. However, if a larger volume of TE buffer is used to resuspend the DNA pellet, or if the ethanol precipitation results in a lower yield than expected, lower dilutions of the Purified end-capped DNA solutions can be required for ODS experiments.
21. In principle, any buffer with a pH of 7.0–8.0, with different monovalent salt (NaCl or KCl) concentrations (0 – 1000 mM), can be employed to generate underwound DNA using ODS. However, owing to the increased stability of the biotin-streptavidin bonds at higher ionic strengths (**30**), it can be more difficult and/or time consuming to prepare the maximum possible  $\sigma$  (*i.e.*,  $\sigma \sim 0.7$ ) at NaCl concentrations  $\gg 150$  mM. For this reason, it is recommended that underwound DNA is generated using the defined ‘ODS buffer’. Once underwound DNA is

prepared in the ODS buffer, it can be moved (at low forces,  $<40$  pN) to other channels in the flowcell that contain buffers with different salt concentrations (including no salt) without any change in  $Lk$  (**14**).

22. In some commercial bead samples, a small number of beads exhibit different sizes and/or shapes than expected, which can alter both the measured force and the apparent DNA end-to-end length. By inspecting the brightfield images of the beads, it should be ensured that both trapped beads are of similar size and shape.
23. When catching DNA between the two beads, if  $D_B$  is  $\ll 10$   $\mu\text{m}$ , there is often a high probability that more than one DNA molecule will be tethered between the two beads. Furthermore, if using a high buffer flow (such that the drag force on Bead 1 is  $>150$  pN), there is often a high probability that one or both beads will be lost from the optical traps.
24. Flow stretching of DNA tethered on one end to Bead 1 allows the other end to tether to Bead 2.
25. The fraction of intact DNA molecules (*i.e.*, without backbone nicks) in optical tweezers experiments typically ranges from 70% to 95%, depending on sample preparation and day-to-day variations in the flow system.
26. If the fraction of nicked DNA molecules is higher than 30%, and there are no air bubbles in the flowcell and no blockages in either the tubing or the valves, the loss of DNA integrity is most likely due to degradation of the DNA sample. In this case, a fresh sample should be prepared, as described in **Subheading 3.1**.
27. If the measured force increases at smaller values of  $D_B$  than anticipated and / or the force plateau occurs at higher forces than expected (*i.e.*,  $\geq 120$  pN), there are at least two DNA molecules tethered between the beads. If this occurs, the tethering of each molecule can sometimes be broken sequentially after waiting at high forces for several seconds / minutes, until only a single DNA molecule remains tethered between the beads. If a single tethered DNA molecule cannot be recovered in this way, discard the beads and tether a new DNA molecule between two new beads. In some cases, the FD-curve of two torsionally unconstrained DNA molecules can look similar to that of a single torsionally constrained DNA molecule. These situations can be differentiated as the onset of the force plateau for the case of two torsionally unconstrained DNA molecules is sharper and the height of the force plateau is higher ( $\sim 120$  pN versus  $\sim 115$  pN).
28. In some cases, torsionally constrained DNA molecules can switch between different biotin-streptavidin binding behaviours (as defined in **Subheading 3.6**). It is relatively common, for example, for a DNA molecule to switch from Type 1 to Type 2 or vice versa during stretching. Molecules displaying Type 3 behaviour can occasionally be converted to Type 2 during



stretching, and also sometimes to Type 1 by waiting at low force ( $<5$  pN) for up to 1 minute before re-stretching. Additionally, torsionally constrained molecules can occasionally switch to an unconstrained state permanently during stretching. This mainly arises from the loss of a biotin-streptavidin bond, but can also occur due to spontaneous formation of a photo-induced or thermal-induced nick in the backbone (*14*). These latter effects are more likely when using higher trapping laser powers.

29. The process of converting end-closed torsionally unconstrained DNA into torsionally constrained DNA, as described in **Subheading 3.6.4**, will typically only be successful if the tethering between the DNA and Bead 2 is broken. In contrast, if the tethering between the DNA and Bead 1 is broken, it is difficult to re-tether the molecule (due to the fact that the flow in our configuration proceeds in the direction of Bead 1 to Bead 2). The end of the DNA molecule that is linked to the beads via a single biotin-streptavidin bond is random and therefore cannot be predicted.
30. When transferring the supercoiled DNA molecule (generated via ODS) from Channel 3 to Channels 4 or 5 for subsequent incubation in other buffer/protein/ligand solutions, it is recommended that  $D_B$  is  $\sim 15$   $\mu\text{m}$ . This distance is usually sufficient to prevent additional DNA molecules (that are tethered to one of the beads via a single end) from becoming tethered between the two beads as a result of flow drag generated during movement. Importantly, this distance is also sufficiently small that any flow drag acting perpendicular to the DNA molecule is not high enough to disrupt the biotin-streptavidin bonds.
31. For proper calibration of the supercoiling density, it is vital that the DNA end-to-end length is calculated accurately. Incorrect values for the pixel size of the CMOS camera (which is used to calculate the bead-bead separation distance) as well as errors in the bead diameter can affect the accuracy of the supercoiling density calibration.

## Figures

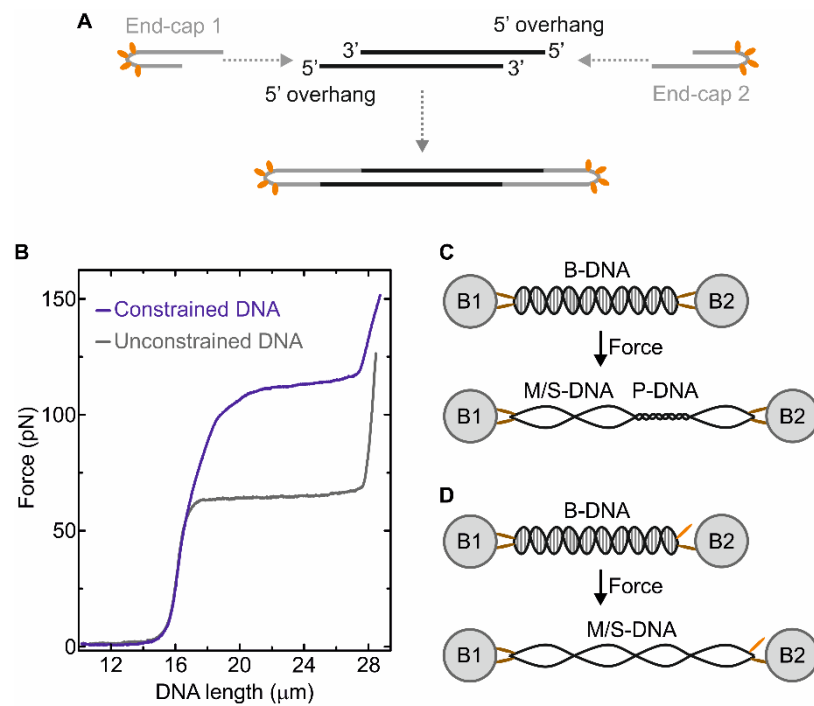


**Figure 1.** Preparation of end-closed torsionally constrained DNA substrates for ODS. **A.** An end-closed DNA molecule is prepared by ligating an ‘end-cap’ to each sticky end of a linear double-stranded (ds)DNA molecule. The end-cap consists of a hairpin structure with a stretch of ssDNA, where the latter is complementary to the overhang of one end of the linear dsDNA. The end-cap has 4 biotin moieties (orange) covalently attached to a 5T-loop at the tip of the hairpin (22). **B.** Representative FD-curves of end-closed torsionally constrained (non-supercoiled)  $\lambda$ -DNA (blue) and end-closed torsionally unconstrained  $\lambda$ -DNA (grey). **C.** Schematic showing the case where the construct in panel A is tethered between two optically-trapped beads (labelled B1 and B2, respectively) via at least two biotin-streptavidin bonds (brown ellipses) on each end of the molecule, resulting in torsionally constrained DNA. Application of tension ( $\sim 115$  pN), induces an overstretching transition, in which the molecule is converted from B-DNA to a combination of overwound DNA (P-DNA) and underwound DNA (in the form of either S-DNA or basepair-melted (M-)DNA) (22,23). **D.** Schematic showing the case where the construct in panel A is tethered between two optically-trapped beads via two biotin-streptavidin bonds on one end, and one biotin-streptavidin bond on the other end. Brown ellipses represent successful biotin-streptavidin bonds; orange ellipses indicate biotin that is not bound to the beads. Application of tension ( $\sim 65$  pN), induces an overstretching transition, in which the molecule is converted from B-DNA to underwound DNA (S-DNA or M-DNA) (21).

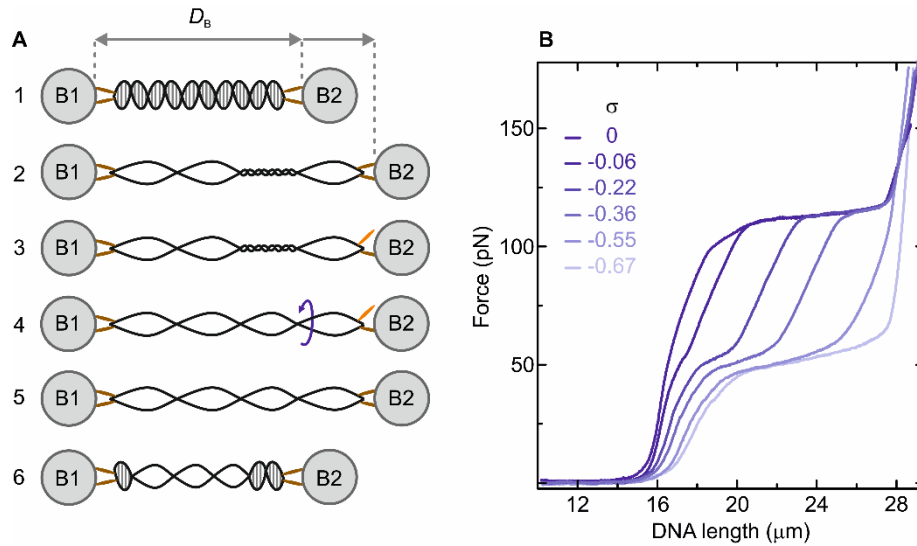


**Figure 2.** Overview of ODS (*14*). **A.** Schematic depicting the principle of ODS, involving 6 key steps. 1) An end-closed DNA molecule is tethered between two optically-trapped beads (labelled B1 and B2, respectively). The distance between the two beads is defined here as  $D_B$ . The DNA is tethered to each bead via at least two biotin-streptavidin bonds (brown ellipses), resulting in a torsionally constrained DNA substrate. 2) The end-closed torsionally constrained DNA is overstretched (see also Fig. 1C), yielding a combination of overwound (P-DNA) and underwound (S-DNA/M-DNA). 3) During overstretching ( $\sim 115$  pN), or at forces  $> 115$  pN, one or more biotin-streptavidin bonds rupture such that at least one end of the DNA is tethered to the respective bead with only a single biotin-streptavidin bond. This results in a loss of torsional constraint. Biotin unbound from streptavidin is depicted by the orange ellipse. 4) The torsional stress is released (either partially or fully) via swivelling of the DNA around the single biotin-streptavidin bond. 5) The broken tether(s) re-form, such that each end of the DNA molecule is once again tethered to the respective bead via at least two biotin-streptavidin bonds. This re-instates torsional constraint, but with a reduced  $Lk$  relative to that of B-DNA. 6) The tension is reduced (to below 40 pN), which stabilizes the tethers and preserves the DNA molecule in an underwound (negatively supercoiled) state for long periods of time (hours). **B.** Representative FD-curves for negatively supercoiled  $\lambda$ -DNA (with different supercoiling densities,  $\sigma$ ), generated via ODS.

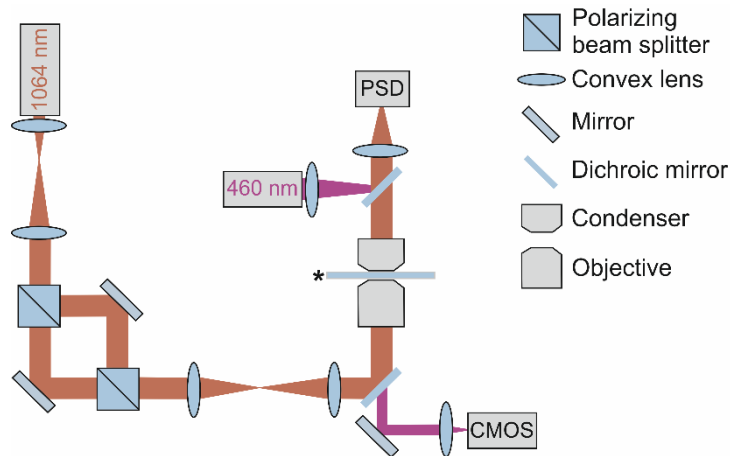


**Figure 3.** Schematic showing the beam paths and essential components of the dual-trap optical tweezers set-up used for ODS. Red lines represent the beam path of the infrared laser light used to generate two optical traps and to measure applied forces. Purple lines indicate the beam path of the LED light used for brightfield illumination of the flowcell. The locations of key optical components (mirrors, polarizing beam splitters, lenses, objective and condenser) are shown in the schematic and identified in the accompanying legend. The following components are also highlighted in the schematic: 1064 nm trapping laser; Position-Sensitive Detector (PSD), used for force detection; LED (460 nm), used for brightfield illumination; CMOS camera, used for acquiring brightfield images. The asterisk highlights the location of the flowcell, which is housed within an automated stage. The design is described in further detail in Reference (18). Figure adapted from Reference (18).

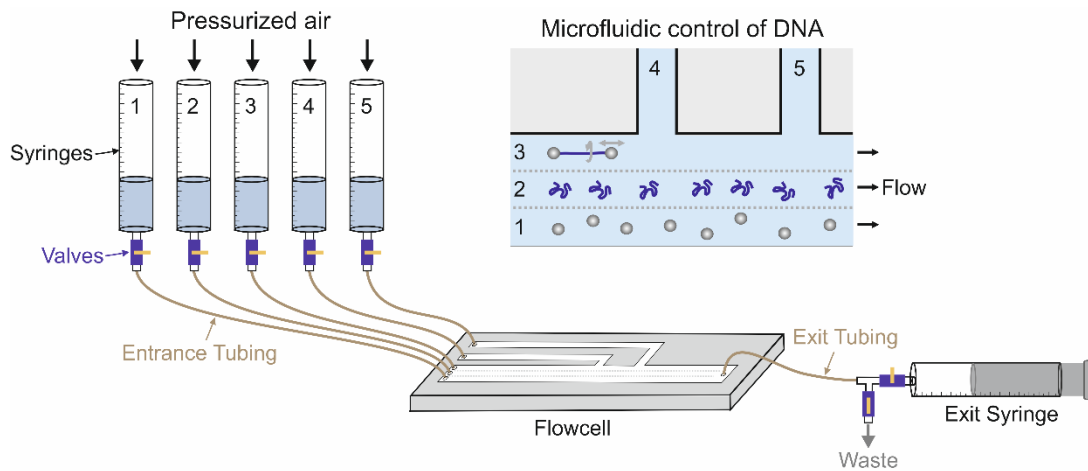


**Figure 4.** Schematic of the flow system used for ODS experiments. Experiments are performed in a glass flowcell that contains 5 inlet channels (Channels 1-5). Solutions are introduced into each inlet channel through a series of ‘entrance’ tubes that are connected, respectively, to inlet syringes (Syringes 1-5). The syringes are held within a pressure box that allows application of up to 3 atm. Fluid flow from these syringes can be blocked using 5 valves (Valves 1-5). Fluid exits the flowcell via a single exit tube, which is connected to either a waste vial or an exit syringe. Typically, beads, DNA and ODS buffer are introduced into Channels 1-3, respectively (see inset). Channels 4 and 5 contain buffer either with or without DNA-binding proteins/ligands. As shown in the inset, Channels 1-3 merge within the flowcell, such that pressure applied to Syringes 1-3 results in laminar flow within the central chamber (indicated by the dashed grey lines). Using this arrangement, two beads can be optically trapped in Channel 1 and moved to Channel 2, where a single DNA molecule is tethered between the beads. The DNA-Beads assembly is then moved to Channel 3, and ODS is performed. Channels 4 and 5 are connected to the central chamber of the flowcell further downstream. Supercoiled DNA generated via ODS can be incubated in DNA-binding proteins/ligands by moving the DNA-Beads assembly into either Channel 4 or 5.

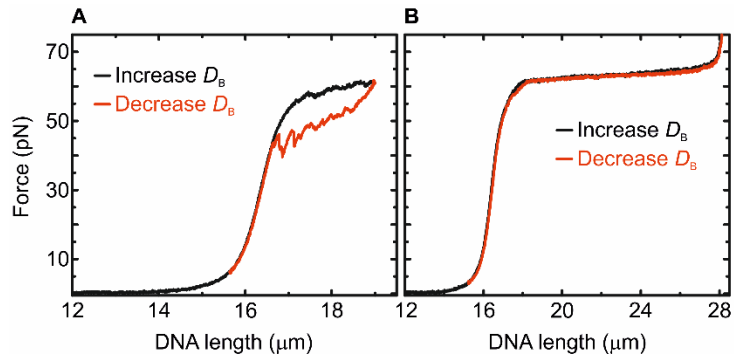


**Figure 5.** Comparison of FD-curves for end-closed torsionally unconstrained  $\lambda$ -DNA with and without nicks. **A.** Under low salt conditions (50 mM NaCl), nicked DNA exhibits a non-smooth overstretching plateau during extension (black) and hysteresis when comparing the extension and retraction (red) FD-curves. **B.** Under low salt conditions (50 mM NaCl), end-closed torsionally unconstrained DNA without nicks shows a smooth overstretching plateau during extension (black) and no hysteresis when comparing the extension and retraction (red) FD-curves (21).

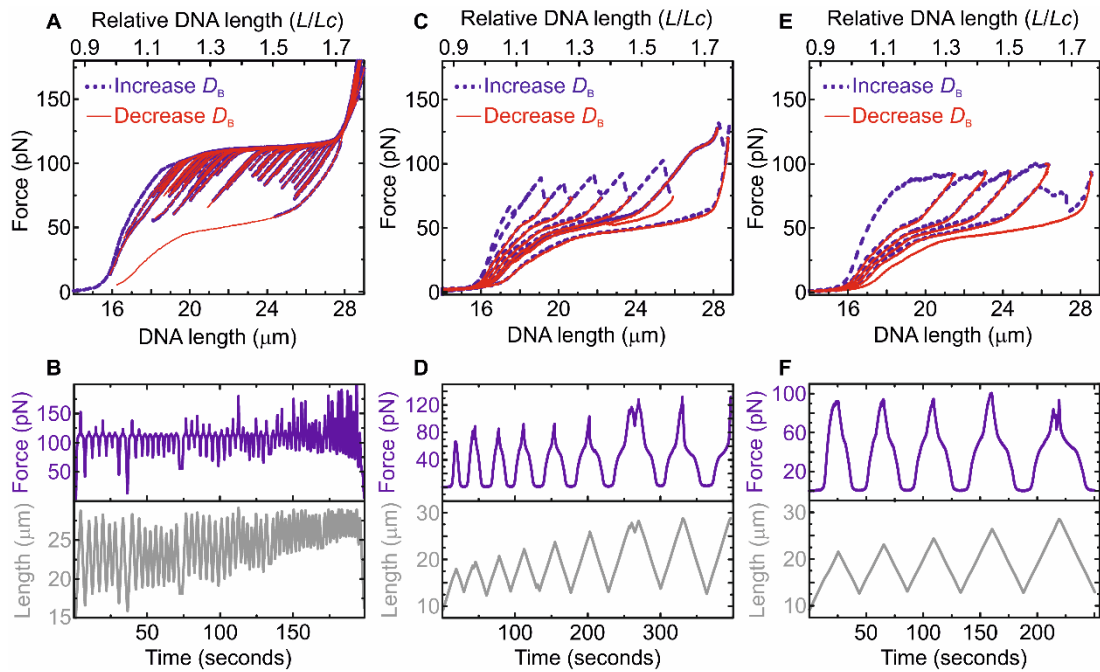


**Figure 6.** Overview of the three main types of behaviour through which a fixed reduction in  $Lk$  is generated by ODS: Type 1 (**A,B**), Type 2 (**C,D**) and Type 3 (**E,F**). In each case,  $D_B$  (see Fig. 2A) is increased and decreased sequentially, resulting in a progressive change in  $Lk$ . Upper panels show the extension (blue) and retraction (red) FD-curves, while the lower panels display the corresponding change in force (purple) and distance (grey) over time. **A,B.** Type 1 molecules are characterized by a smooth overstretching plateau at  $\sim 115$  pN. A fixed change in  $Lk$  is typically observed after first extending the molecule beyond the end of the overstretching plateau, waiting for a fixed period of time (*e.g.*, 10 seconds) and then reducing  $D_B$ . By recording many sequential extension-retraction curves (each one inducing a small fixed change in  $Lk$ ), a wide range of supercoiling densities (with  $\sigma$  between 0 and  $\sim -0.7$ ) can be generated (**I4**). This can be appreciated in panel A by the increasing shift in the resulting FD-curves after each extension-retraction cycle. **C,D.** Type 2 molecules exhibit large and sudden force ruptures in the extension FD-curve between  $\sim 1.1 Lc$  and  $1.75 Lc$ . A fixed reduction in  $Lk$  is generated after each rupture, as revealed by the subsequent retraction FD-curve. The magnitude of  $\sigma$  (ranging from 0 to  $\sim -0.7$ ) is directly proportional to the distance at which the force rupture occurs. **E,F.** Type 3 molecules display a rough force plateau as the end-to-end length is increased from  $\sim 1.1 Lc$  to  $1.75 Lc$ . In these molecules, the magnitude of  $\sigma$  generated is directly proportional to the extent to which the DNA molecule is extended (over the range of  $\sim 1.1 Lc$  to  $1.75 Lc$ ) (**I4**). Data shown here are for  $\lambda$ -DNA.

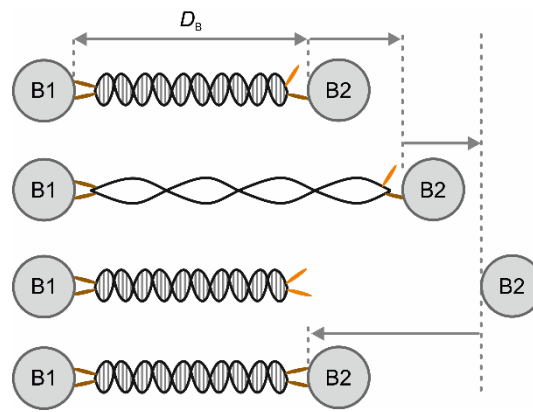


**Figure 7.** Schematic depicting a procedure to convert end-closed DNA from a torsionally unconstrained state to a torsionally constrained state. Here, the DNA is assumed to be connected to Bead 1 (B1) via two biotin-streptavidin bonds and to Bead 2 (B2) through only a single tether (and thus is torsionally unconstrained). Progressively increasing  $D_B$  by moving Bead 2 initially overstretches the unconstrained molecule and eventually leads to the permanent rupture of the single tether between the DNA and Bead 2. Reduction of  $D_B$ , along with application of fluid flow (in the direction of Bead 1 to Bead 2), induces the re-attachment of the DNA molecule to Bead 2. In many cases, this re-attachment involves at least two biotin-streptavidin bonds, and thus the DNA molecule is now torsionally constrained. ODS can then be performed on this molecule. Successful tethers are depicted by brown ellipses; biotin unbound from streptavidin is indicated by orange ellipses.



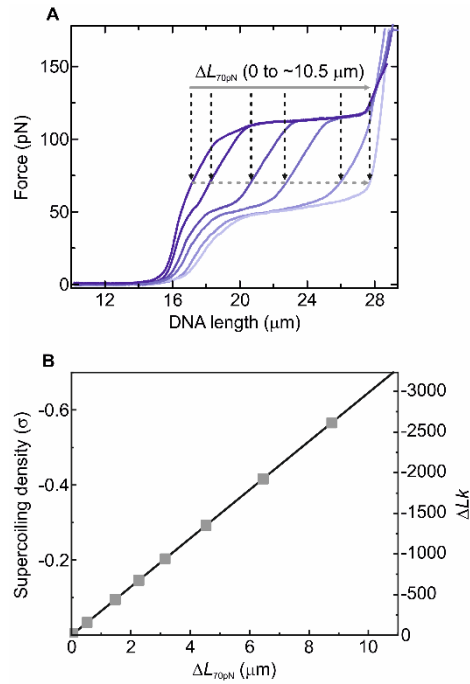


**Figure 8.** Procedure for calibrating the supercoiling density ( $\sigma$ ) generated by ODS. **A.** FD-curves for different values of  $\sigma$ , in which the difference in DNA end-to-end length relative to that of non-supercoiled torsionally constrained DNA at 70 pN (defined as  $\Delta L_{70\text{pN}}$ ) is highlighted. **B.** Calibration plot showing the increase in  $\Delta L_{70\text{pN}}$  as a function of  $\sigma$ , as determined from literature FD-curves of negatively supercoiled DNA (23). Data are fit with a linear function (14). The value of  $\sigma$  for FD-curves obtained using ODS is then determined by correlating the measured value of  $\Delta L_{70\text{pN}}$  with the corresponding  $\sigma$ , based on the calibration plot in panel B.

## **Acknowledgements**

We thank Federica Burla for critical input and support on the development of ODS, Andreas Biebricher for valuable discussions and Nikolai Born for experimental assistance. We are also grateful for financial support from a Chemical Sciences Top grant from the Netherlands Organization for Scientific Research (G.J.L.W, E.J.G.P and G.A.K).

## **Competing interests**

The Optical DNA Supercoiling method described in this chapter is the subject of a patent application, licensed to LUMICKS B.V., in which G.A.K, E.J.G.P. and G.J.L.W. have a financial interest.

## References

---

- <sup>1</sup> Naughton C et al (2013) Transcription forms and remodels supercoiling domains unfolding large-scale chromatin structures. *Nat Struct Mol Biol* 20:387–395
- <sup>2</sup> Ma J, Bai L, Wang MD (2013) Transcription under torsion. *Science* 340:1580–1583
- <sup>3</sup> Champoux JJ (2001) DNA topoisomerases: Structure, function, and mechanism. *Annu Rev Biochem* 70:369–413
- <sup>4</sup> Koster DA, Crut A, Shuman S, Bjornsti M-A, Dekker NH (2010) Cellular strategies for regulating DNA supercoiling: A single molecule perspective. *Cell* 142:519–530
- <sup>5</sup> Sinden RR, Carlson JO, Pettijohn DE (1980) Torsional tension in the DNA double helix measured with trimethylpsoralen in living *E. coli* cells: Analogous measurements in insect and human cells. *Cell* 21:773–783
- <sup>6</sup> Wang JC (2002) Cellular roles of DNA topoisomerases: A molecular perspective. *Nat Rev Mol Cell Biol* 3:430–440
- <sup>7</sup> Szczelkun MD et al (2014) Direct observation of R-loop formation by single RNA-guided Cas9 and Cascade effector complexes. *Proc Natl Acad Sci USA* 111:9798–9803
- <sup>8</sup> Newton MD et al (2019) DNA stretching induces Cas9 off-target activity. *Nat Struct Mol Biol* 26:185–192
- <sup>9</sup> Ivanova IE, Wright AV, Cofsky JC, Palacio Arisd KD, Doudna JA, Bryant Z (2020) Cas9 interrogates DNA in discrete steps modulated by mismatches and supercoiling. *Proc Natl Acad Sci USA* 117:5853–5860
- <sup>10</sup> Bryant Z et al (2003) Structural transitions and elasticity from torque measurements on DNA. *Nature* 424:338–341
- <sup>11</sup> La Porta A, Wang MD (2004) Optical torque wrench: Angular trapping, rotation, and torque detection of quartz microparticles. *Phys Rev Lett* 92:190801–190804
- <sup>12</sup> Deufel C, Forth S, Simmons CR, Dejgoshia S, Wang MD (2007) Nanofabricated quartz cylinders for angular trapping: DNA supercoiling torque detection. *Nat Methods* 4:223–225
- <sup>13</sup> Seol Y, Neuman KC (2016) The dynamic interplay between DNA topoisomerases and DNA topology. *Biophys Rev* 8:S101–S111
- <sup>14</sup> King GA, Burla F, Peterman EJG, Wuite GJL (2019) Supercoiling DNA optically. *Proc Natl Acad Sci USA* 116:26534–26539
- <sup>15</sup> Schakenraad K et al (2017) Hyperstretching DNA. *Nat Commun* 8:2197
- <sup>16</sup> Moffitt JR, Chemla YR, Smith SB, Bustamante C (2008) Recent advances in optical tweezers. *Annu Rev Biochem* 77:205–228
- <sup>17</sup> Heller I, Hoekstra TP, King GA, Peterman EJG, Wuite GJL (2014) Optical tweezers analysis of DNA–protein complexes. *Chem Rev* 114:3087–3119
- <sup>18</sup> Sarlós K et al (2018) Reconstitution of anaphase DNA bridge recognition and disjunction. *Nat Struct Mol Biol* 25:868–876
- <sup>19</sup> Wasserman MR et al (2019) Replication fork activation is enabled by a single-stranded DNA gate in CMG helicase. *Cell* 178:600–611
- <sup>20</sup> van Mameren J et al (2011) Unraveling the structure of DNA during overstretching by using multicolor, single-molecule fluorescence imaging. *Proc Natl Acad Sci USA* 106:18231–18236

- 
- <sup>21</sup> King GA, Gross P, Bockelmann U, Modesti M, Wuite GJL, Peterman EJG (2013) Revealing the competition between peeled-ssDNA, melting bubbles and S-DNA during DNA overstretching using fluorescence microscopy. *Proc Natl Acad Sci USA* 110:3859–3864
- <sup>22</sup> King GA, Peterman EJG, Wuite GJL (2016) Unravelling the structural plasticity of stretched DNA under torsional constraint. *Nat Commun* 7:11810
- <sup>23</sup> Léger JF et al (1999) Structural transitions of a twisted and stretched DNA molecule. *Phys Rev Lett* 83:1066–1069
- <sup>24</sup> Pincet F, Husson, J (2005) The solution to the streptavidin-biotin paradox: The influence of history on the strength of single molecular bonds. *Biophys J* 89:4374–4381
- <sup>25</sup> Gruber S, Löf A, Sedlak SM, Benoit M, Gaub HE, Lipfert J (2020) Designed anchoring geometries determine lifetimes of biotin–streptavidin bonds under constant load and enable ultra-stable coupling. *Nanoscale* 12:21131–21137
- <sup>26</sup> Gittes F, Schmidt CF (1998) Signals and noise in micromechanical measurements. *Methods Cell Biol* 55:129–156
- <sup>27</sup> Moffitt JR, Chemla YR, Izahky D, Bustamante C (2006) Differential detection of dual traps improves the spatial resolution of optical tweezers. *Proc Natl Acad Sci USA* 103:9006–9011
- <sup>28</sup> Simmons RM, Finer JT, Chu S, Spudich JA (1996) Quantitative measurements of force and displacement using an optical trap. *Biophys J* 70:1813–1822
- <sup>29</sup> Peterman EJG, Gittes F, Schmidt CF (2003) Laser-induced heating in optical traps. *Biophys J* 84:1308–1316
- <sup>30</sup> Holmberg A, Blomstergren A, Nord O, Lukacs M, Lundeberg J, Uhlén M (2005) The biotin-streptavidin interaction can be reversibly broken using water at elevated temperatures. *Electrophoresis* 26:501–510
- <sup>31</sup> Nichols BP, Donelson JE (1977) 178-nucleotide sequence surrounding the cos site of bacteriophage lambda DNA. *J Virol* 26:429–434
- <sup>32</sup> Paik DH, Perkins TT (2011) Overstretching DNA at 65 pN does not require peeling from free ends or nicks. *J Am Chem Soc* 133:3219–3221
- <sup>33</sup> Gittes F, Schmidt CF (1998) Interference model for back-focal-plane displacement detection in optical tweezers. *Opt Lett* 23:7–9
- <sup>34</sup> Neuman KC, Nagy A (2008) Single-molecule force spectroscopy: Optical tweezers, magnetic tweezers and atomic force microscopy. *Nat Methods* 5:491–505
- <sup>35</sup> Allemand JF, Bensimon D, Lavery R, Croquette V (1998) Stretched and overwound DNA forms a Pauling-like structure with exposed bases. *Proc Natl Acad Sci USA* 95:14152–14157
- <sup>36</sup> Ganji M, Hyun Kim S, van der Torre J, Abbondanzieri E, Dekker C (2016) Intercalation-based single-molecule fluorescence assay to study DNA supercoil dynamics. *Nano Lett* 16:4699–4707
- <sup>37</sup> Joo C, Ha T (2012) Preparing sample chambers for single-molecule FRET. *Cold Spring Harb Protoc* 7:1104–1108
- <sup>38</sup> Brouwer I, King GA, Heller I, Biebricher AS, Peterman EJG, Wuite GJL (2017) Probing DNA–DNA interactions with a combination of quadruple-trap optical tweezers and microfluidics. In *Optical Tweezers: Methods and Protocols, Methods in Molecular Biology*, Springer 1486:275–293